Measurement 186 (2021) 110170

Contents lists available at ScienceDirect

Measurement

journal homepage: www.elsevier.com/locate/measurement

Imaging and simulations of positive surface and airborne streamers adjacent to dielectric material

Marek Florkowski

AGH University of Science and Technology, Al. Mickiewicza 30, 30-059 Krakow, Poland

ARTICLE INFO

Keywords:
Imaging
Streamer
Partial discharges
Phase-resolved measurements
High voltage

ABSTRACT

This paper presents the imaging and simulations of positive airborne and surface streamers in the air that is adjacent to a dielectric material. The goal of this paper is to investigate the intriguing observation of the occurrence of airborne streamers that originate at a dielectric surface at a distance from the tip of a high-voltage electrode. This effect may be attributed to the accumulation of charges at a spot on the dielectric material during subsequent streamers. Such a positively charged spot causes airborne streamer inception after reaching the critical value of the charge density. This effect is observed in a side-view configuration by high-speed imaging in a time-accumulated and spatially resolved mode. The hypothesis of the occurrence of airborne streamers in certain sequences was complemented by 2D simulations. The surface charge densities were quantitatively evaluated by the simulations. Two types of streamers were simulated: first – without an accumulated surface charge; and second – with a spot of a defined charge density (which triggers the airborne streamer). After reaching the critical value of the charge density, such spots that are charged during subsequent cathode-directed streamer events may trigger a discharge towards the air side. The length of the surface streamer along the dielectric surface is voltage-dependent. The experimental and simulation results extend the insight to streamer mechanism in configurations with charges accumulated on the dielectric surface – including the inception of an airborne streamer.

1. Introduction

In the high voltage electrical generation, transmission, distribution constructions and in emerging areas such as renewable photovoltaic or even e-mobility (where the strive towards higher voltage is expected) as well in biomedical processes and applications that involve plasma [1], the crucial element from the electric insulation point of view is the gas-dielectric-metal interface (which is often called a tipple junction point). This interface is associated with surface discharges under certain conditions, which may lead to insulation deterioration in the form of erosions or even flashovers. These are important for power equipment's reliability and long-term endurance. The discharge development is related to so-called streamer inception, formation, and development. Streamers are usually defined as a tiny channels of ionized gas. The physics of streamers is an important area of electrical discharges in gases. There has been a lot of research with respect to streamer measurement [e.g., [1–5]] and streamer modeling [e.g., [6–17]] – especially in the last few decades. In general, the research refers to both positive (cathode-directed) and negative streamer development. Inception of streamer discharges starts typically in a highly non-uniform electric field. Then, they may propagate into a region that has a background electric field below the breakdown level. For decades [2–4], a streamer has been described and visualized as a fast-moving head that propagates as an ionization wave and leaves an ionized tail behind [1,14]. During the propagation of a streamer channel, various forms of branches and filaments are usually observed. The random spatial branching is attributed to the fluctuations of electron density in the region in front of a streamer head as well as the presence of space charges [14]. In the last few decades, strong development has also been observed in fast streamer imaging [18–24]. A streamer's development is usually analyzed in air, SF_6, or gas mixtures [25–28]. Usually, the test arrangement is point-plate and streamer development in bulk gas is analyzed. With respect to practical implementations, an important configuration is also a setup with surface discharges along the dielectrics [29–31]. Surface streamers may further lead to flashovers under certain condition, thus creating dangerous effects in terms of high-voltage (HV) electrical insulation. It has also been noticed that the presence of a surface decreases the breakdown voltage in an atmospheric environment [5,29,32]. Those

E-mail address: marek.florkowski@agh.edu.pl.

https://doi.org/10.1016/j.measurement.2021.110170
Received 21 July 2021; Received in revised form 10 September 2021; Accepted 12 September 2021
Available online 16 September 2021

streamers that develop adjacent to a surface are involved in several processes, which is the subject of ongoing research worldwide. Depending on the materials, electrode configurations, or composition of the gaseous environments, these refer to the investigations of the interplay of streamer development and its associated charge trapping, secondary electron emission, and the emission of photoelectrons. There are various interpretation of these effects as well as the impact of a dielectric surface on streamer development [1–5]. The possible occurrence of two streamer phases (air and surface) has also been suggested [29,32]. In this work, the measurements and simulations of positive cathode-directed surface and airborne streamers that are propagated in the presence of an adjacent dielectric surface in atmospheric air are reported. The coexistence of the surface and airborne streamers is presented. An especially intriguing observation of the occurrence of airborne streamers that originate at a dielectric surface at a distance from the tip of a high-voltage electrode are also investigated. Paper extends the knowledge and presents hypothesis about the origin of the airborne streamer as an effect of the surface charge accumulation. This effect was observed experimentally and is explained by simulations in the paper.

2. Surface streamer discharges

One of the most typical forms of discharges are surface discharges. The initiation of a surface streamer is usually focused around a triple junction. Several theories have been elaborated regarding electrons traveling along a dialectic surface [30,33,34], such as a secondary electron emission avalanche, an electron cascade, or an electron strike surface in a vacuum. It has been observed [30] that a single avalanche can only charge within nanoseconds on a narrow strip; thus, many streamers may be required to achieve a final surface charge state. Significant research has been carried out on the influence of previous positive streamers on discharge propagation [35–38], including electrodeless initiated discharges [39]. The discharge transitions are often attributed to the memory effects that are associated with residual accumulated charges [40–46]. Significant influence on the streamer propagation along a dielectric surface have material properties, especially permittivity [13,33,34,47].

The positive streamers move in an opposite direction to the electron drift. In this context, a source of the electrons that are in front of the streamer head is required for cathode-directed streamer propagation. Hence, the positive streamer growth depends not only of the local electric field but also on the electron density in a head forefront [48]. There are various methods for modeling this aspect – either as a complex photoionization mechanism or as background ionization [49–51]. The coefficients of ionization α and attachment η are required, which are modified by the presence of a dielectric surface. As proposed in [32], two effects may occur:

- The surface emits electrons due to photon bombardment. This may contribute to both the supply of avalanche-initiating electrons (increasing photoionization) and to the bulk ionization in the avalanche (contributing to the collisional ionization).
- The surface may attach electrons in surface traps and positive ions by electrostatic attraction, thus causing an additional attachment to the one in the gas. It was thus postulated that the ionization and attachment coefficients that control the streamer propagation along a dielectric surface are higher than those in air.

For surface discharges, photo electron emission from the insulator surface can contribute in a surface-adjacent layer to the photoionization of the oxygen molecules in the bulk streamer discharges [52]. Some researchers have associated this effect with the resulting speed of the streamers, which are faster at the surface as compared to the bulk penetration [13,53,54].

The positive streamer propagates due to the strong electric field gradient in the tiny head layer of the space charge; this maintains the ionization process, as the electrons in this case are sucked backwards by a streamer stem. The photoionization in air is usually explained as the interplay between the nitrogen and oxygen processes [49]. The accelerated electrons excite the nitrogen atoms by the impact through the strong electric field in the streamer head. N_2 possesses higher ionization energy that oxygen (15.6 eV vs. 12.8 eV); thus, an excited nitrogen molecule can emit a photon and ionize an oxygen molecule. The electrons can be also obtained by detachment from negative ions through collisions or background ionization. The electrons obtained from background ionization are used in this paper in the simulation section, which includes research, modeling, and simulations (including measurement verification from the last decade especially) [1,13,14,26,34,35,38,48,51,52] on positive streamers. The faster propagation of positive streamers was observed and explained with respect to negative ones in [13,49,52,54].

A streamer's development along a dielectric surface is a complex problem that involves the impact of the dielectric materials, the composition of gases, and the electric field, among others. It was observed in [29] that, in the presence of a dielectric surface on a nitrogen atom, the electrons that impact the surface will be trapped in the bulk of the dielectric. In this case, this energy is still below the first crossover point for secondary electron emission and refers to the impacting electrons. Therefore, the electrons that hit the dielectric surface are trapped in the bulk of the material. In nitrogen, such an electron lacks the necessary energy for liberating the secondary electrons from the surface and are therefore trapped by the material surface. However, as reported in [29], the case is different for air with its oxygen content. In this case, a positive surface charge is present due to photoemission. It was stated that the elevated UV presence in the excited air is releasing electrons from the material surface, resulting in a net positive charge that attracts the electron avalanche head; this causes a streamer to propagate close to the surface. In air, enhanced photoemission is observed due to its UV intensity (which is higher than it is in nitrogen). In the case of energy that is too low for secondary electron emission, an absorption of the electrons by the surface will occur, resulting in surface charging. Thus, it may be stated that, the level of oxygen concentration of the environment determines whether the adsorption of the electrons by the dielectric surface or photoemission dominates in determining the surface charge [55]. There is still a lot of ongoing research into which mechanism i.e. the attraction or repulsion of the electrons by the surface charges or the photoemission effect from the surface as a supplementary mechanism of electron origin in the gas is dominant.

Surface discharges that propagate on the dielectric material over a long period of time may cause erosion and insulation degradation; this can lead to a potential flashover at a certain stage. There are various methods for assessing the condition of the insulation. Recently, tracing hyperspectral imaging has also been applied for deterioration, creating an interesting approach for diagnostic applications [56].

3. Experimental setup and measurement methodology

The experimental setup was designed to record the sequence of streamers that propagated adjacent to an dielectric surface. Consisting of optical imaging and electrical discharge recording, the experimental configuration and measuring instrumentation is described below. Cathode-directed streamers developed at the tip of a high-voltage electrode. The sinusoidal high-voltage waveform was applied to trigger a sequence of streamers on the positive rising part of the waveform (half-period, angle 0°–180°). A frequency of 4 Hz was selected to make it possible to continuously record the discharges over consecutive periods without time gaps. The voltage and interelectrode distance were tuned to achieve streamer development along the dielectric surface but not bridging the electrodes, thus failing to reach the cathode. The voltage magnitude was adjusted up to 20 kV. The partial discharge (PD) inception voltage in the presented configuration was observed at 6.8 kV.

In this way, cathode-directed streamers are generated above this threshold value. For an individual streamer event with a duration of several dozen nanoseconds, the voltage can be treated as a constant. The camera was adjusted for the synchronous imaging of streamers within a half-period. In this way, the superposition of the streamers was obtained.

3.1. Experimental configuration

The experimental setup is presented in Fig. 1. This configuration reflects the phenomena that occur on the surface of various high-voltage insulators designs (including GIS - Gas Insulated Switchgear and GIL - Gas Insulated Lines spacers). The experiments were performed on the specimens made of epoxy material (depicted in yellow), which was placed in an inclined position with a tilt angle of $\alpha = 45^{\circ}$. The high voltage point electrode, sticking to the dielectric material, is fixed above the grounded planar plate. The electric permeability of the dielectric material was $\varepsilon_r = 5$. The experiments were performed with a dielectric plate with a thickness of 1 mm (there were plates with various thickness tested, down to the 0.3 mm). The distance $a = 20$ mm was set between the HV point and plate electrodes. The point electrode's tip had a spherical radius of $r = 50$ μm. The investigations were done at room temperature under standard conditions; i.e., at an atmospheric pressure of ca. 0.1 MPa.

The cross section geometry of the setup configuration in the side-view shown in Fig. 1 is also utilized for the streamer propagation simulations and calculations of electric field distribution. To provide unified initial conditions, the dielectric specimens were neutralized prior to the experiments to avoid polarization effects and to discharge possible accumulated surface charges. In this way, only untreated samples were exposed.

3.2. Instrumentation of discharge imaging and PD phase-resolved measurement

The streamers that were adjacent to the dielectric surface were observed by an iCCD camera that was positioned at a side view with respect to the specimen [57,58]. The experimental setup and instrumentation is shown in Fig. 2. In the experiments, an imaging equipment composed of high speed camera Andor iCCD (model iSTAR DH334) was applied. The system consists of CCD matrix with a resolution of 1024 × 1024 pixels. A quantum efficiency of an applied optical intensifier was within a spectral range between 200 nm and 850 nm. The applied optical lens system consisted of a UV lens (Ricoh model FL-BC2528) having a focal length of 25 mm. For fine adjustment and strong focus on a streamer spot, the set of extension rings with a distance up to 10 mm were placed in the optical system. Since at AC voltage, a distinctive time stamp is zero crossing of HV waveform, this signal was used for synchronization of the optical part and triggering PD phase-resolved measurements, including phase correction. The supervision of HV waveform was performed by means of a Tekprobe (type P6015), with a built in compensated HV divider one to one thousand.

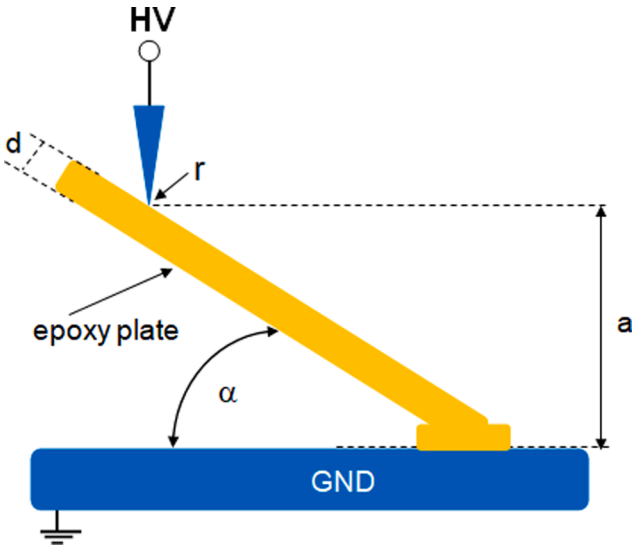

Fig. 1. Configuration of experimental setup for side-view streamer imaging: α - angle of tilt; a – distance between point and planar electrode; d – epoxy plate thickness; r – tip radius.

A notable improvement of the sensitivity of optical measurements (by reduction of the background influence) was achieved placing the system in a darkroom. In this configuration the gain factor of iCCD camera was set to 4000. The imaging was performed during the gate signal in on state and exposition time was adjusted to the duration of a half-period of the high voltage (i.e., to 125 ms at 4 Hz) and retriggered at the positive zero crossing. A sinusoidal high voltage waveform was supplied by HV amplifier (type Trek Model 20/20B) driven by a signal generator (Tektronix AFG 3011) with a programmable waveform. The protection resistor Z was placed upstream in the high voltage path. The coupling capacitor C_k, placed in a parallel branch to the specimen, was closing the PD loop. The camera triggering signal was obtained from a digital delay line (type SR-DG645 by Stanford Research) controlled by a Tektronix AFG3011 signal generator. The measurement acquisition was executed for a defined number of frames. The wideband partial discharges acquisition was done in phase-resolved mode (PRPD) by means of Power Diagnostix's ICMSystem controlled via GPIB interface by a host computer. The digital delay output signal was used for PD synchronization. In an electrical mode PD were picked up by a wideband current transformer, which is represented as CT1 in Fig. 2. The line termination of HF coil was 50 Ω. The experiments were accomplished at following environmental conditions in air having pressure 997 hPa, humidity level 29% and external temperature in the laboratory 22 °C.

4. Surface and airborne streamer imaging

The electrical PD detection and fast imaging were implemented to analyze the surface discharges in air.

The special attention was on the investigations and distinctions between the direct surface adjacent streamers and the airborne ones. For this purpose, the camera was positioned at a side view. The acquisition of discharges was defined in the positive voltage half-period. The PD pulses and spatially resolved optical images were synchronously recorded above the inception voltage. The discharge activity begins with the propagation of weak emissions from the HV needle-tip in the form of tiny filaments. An illustration of the acquisition modes is shown in Fig. 3. In a continuous sinusoidal sequence where the imaging is performed, the positive half-periods are marked by red bars.

Each frame in this visualization provides a superposition of the streamers that occurred during a half-period of the high voltage (i.e., time-accumulated imaging).

The frequency of the high voltage was tuned to 4 Hz to obtain a continuous gapless sequence of surface discharges. The corresponding accumulated phase-resolved PD pattern (shown below) was obtained within 300 s and represents the profile and density of the discharges with respect to the phase angle of the applied voltage. Hence the PRPD image represents the accumulated discharge collection over the entire measurement time. Since the duration of the individual streamers last for tens of nanoseconds, the voltage level (waveform period T = 250 ms) can be assumed to be constant during the streamer development time at the sinusoidal waveform. The magnitude of the HV was adjusted with respect to the length of the surface discharges (which should reach approximately half of the interelectrode distance along the dielectric surface). An exemplary sequence of the cathode-directed streamers that were acquired in the configuration presented in Fig. 2 is presented in

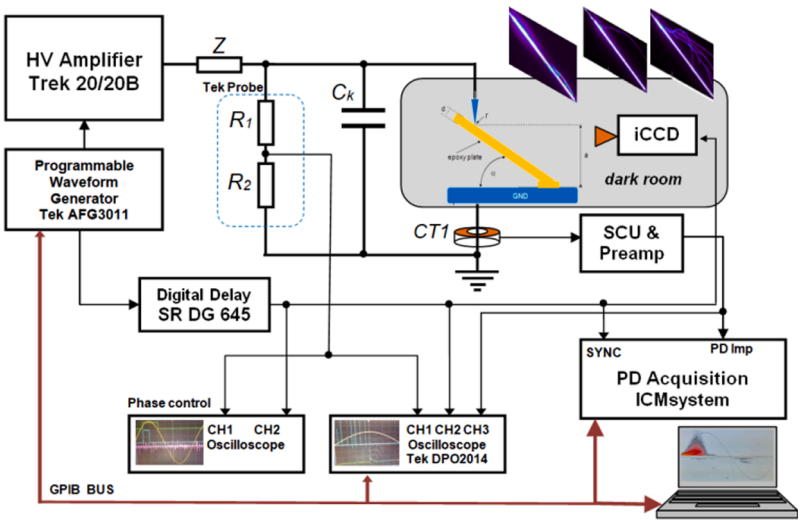

Fig. 2. Instrumentation for surface and airborne streamer imaging and electrical partial discharge recording.

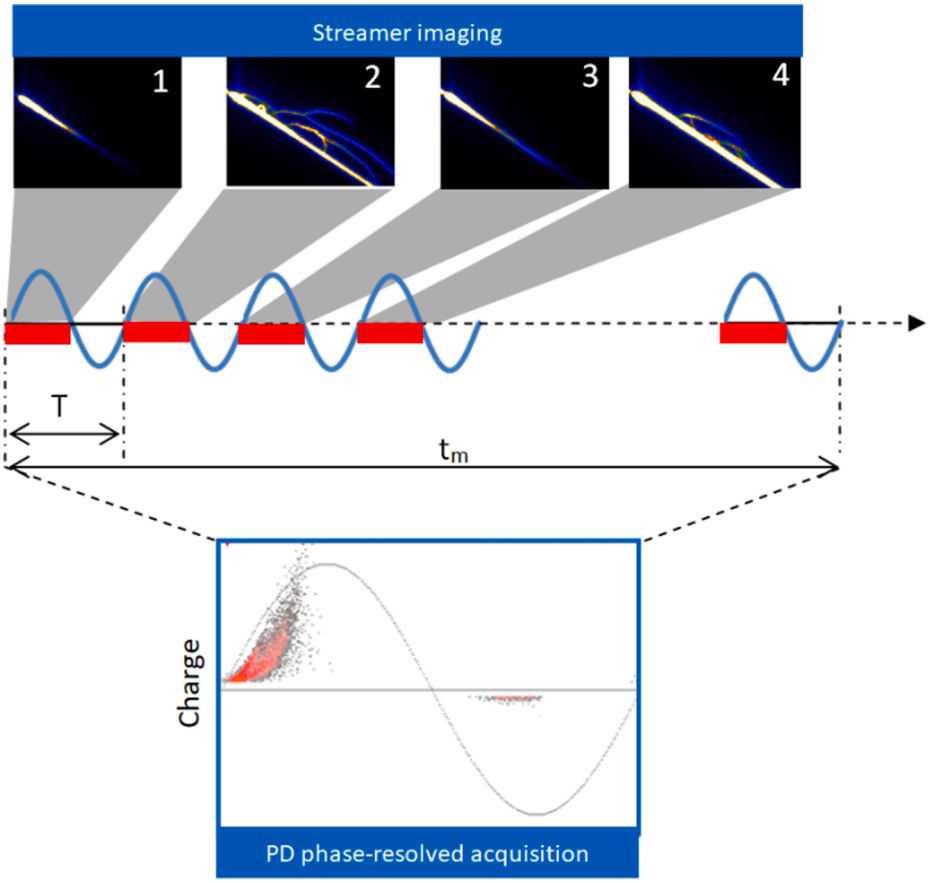

Fig. 3. Illustration of streamer imaging (upper part – light intensity) and PD phase-resolved acquisition (lower part – charge distribution) modes: T – period of high voltage; t_m – measurement time.

Fig. 4. The tip of the high voltage electrode is denoted in the first frame. The 20 continuous frames represent the accumulated view of the streamers during consecutive positive half-periods of the sinusoidal high-voltage stimuli. As shown in the consecutive sequence presented in Fig. 4, surface streamers are visible in all frames; however, airborne streamers are also present in certain frames.

The occurrence and mechanism of the airborne streamers is the focus of this paper. Since the observation is from the side view, the filaments start from the point tip and propagate in various directions towards the plate, creating a time- and spatially-accumulated cross section. In this way, the transition between the discharge modes (i.e., surface-adjacent and airborne streamers) can be observed.

At a certain stage, there is a characteristic formation of a stem. The stem acts like the prolongation of a tip, and stem-branched streamers with tree-like filaments are observed at the stem forefront in the camera's front view (shown in [57]). An exemplary visualization of the

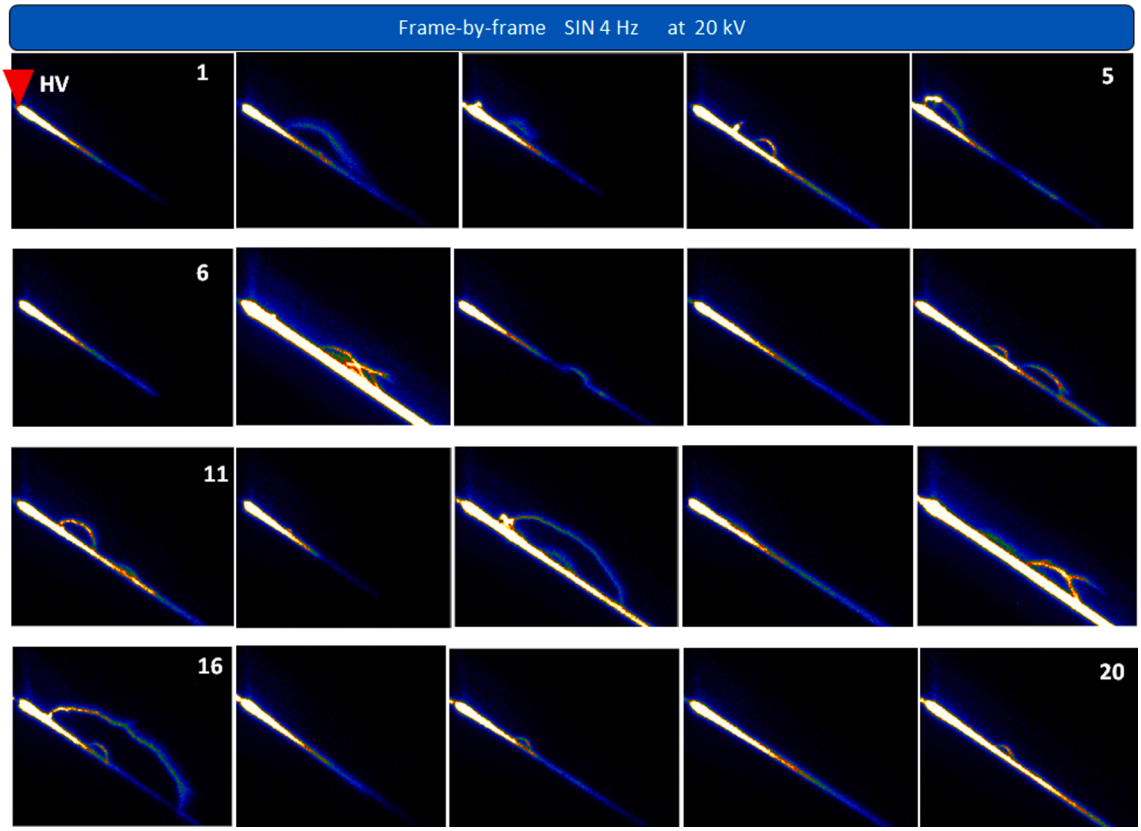

Fig. 4. Sequence (20 consecutive frames) of cathode-directed streamers, frame-by-frame during positive half-period of high voltage (SIN, 20 kV, 4 Hz); tip of HV electrode denoted in first frame.

surface and airborne streamers is shown in the images in Fig. 5. The high-voltage electrode is marked by a red triangle, and the epoxy plate is denoted by a yellow line. This sequence is a superposition of several streamers that occurred on the rising positive part of a high-voltage waveform. The majority of the streamers are surface-adjacent, which is highlighted by a strong surface illumination. The HV electrode-originating airborne streamer is shown in Fig. 5a. Two airborne streamers that are triggered at a distance from the HV electrode are visualized in Fig. 5b.

The first manifests the smaller deflection that started at a greater distance from the needle-tip, whereas the second one (revealing a much longer spread and greater distance from the surface) originated closer to the high-voltage electrode. One of the origin hypotheses of airborne streamers may be attributed to the accumulated surface charge during the sequence and will be elaborated in simulations and in the results discussion section. The focus of this paper is on the origin of the airborne streamers that are triggered at a distance from the HV electrode on the dielectric surface (Fig. 5b). Since the experiments were performed with a sinusoidal voltage, a phase-resolved partial discharge acquisition was possible. The frequency was adjusted to 4 Hz to safeguard the period-by-period PRPD recording synchronously with the imaging using the iCCD camera (gate – 125 ms). The correspondence of the PD phase-resolved patterns and optical images as an evolution function of the supply voltage is presented in Fig. 6 [57].

The voltage was changed from the PD inceptions that were detected from 6.8 kV up to 20 kV. Presence of only surface streamers was noticed

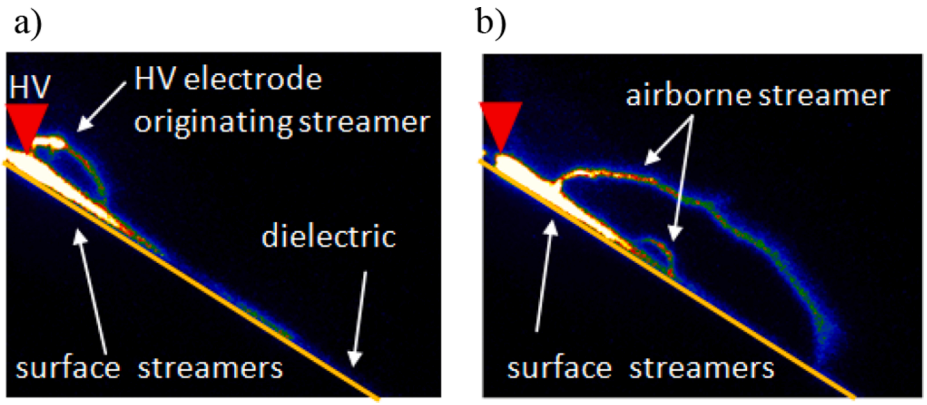

Fig. 5. Accumulated cathode-directed streamers in presence of dielectric surface during half-period at 4 Hz: a) HV electrode originating streamers; b) airborne streamers. High-voltage electrode is marked by red triangle, and epoxy plate is denoted by yellow line (side view). (For interpretation of the references to colour in this figure legend, the reader is referred to the web version of this article.)

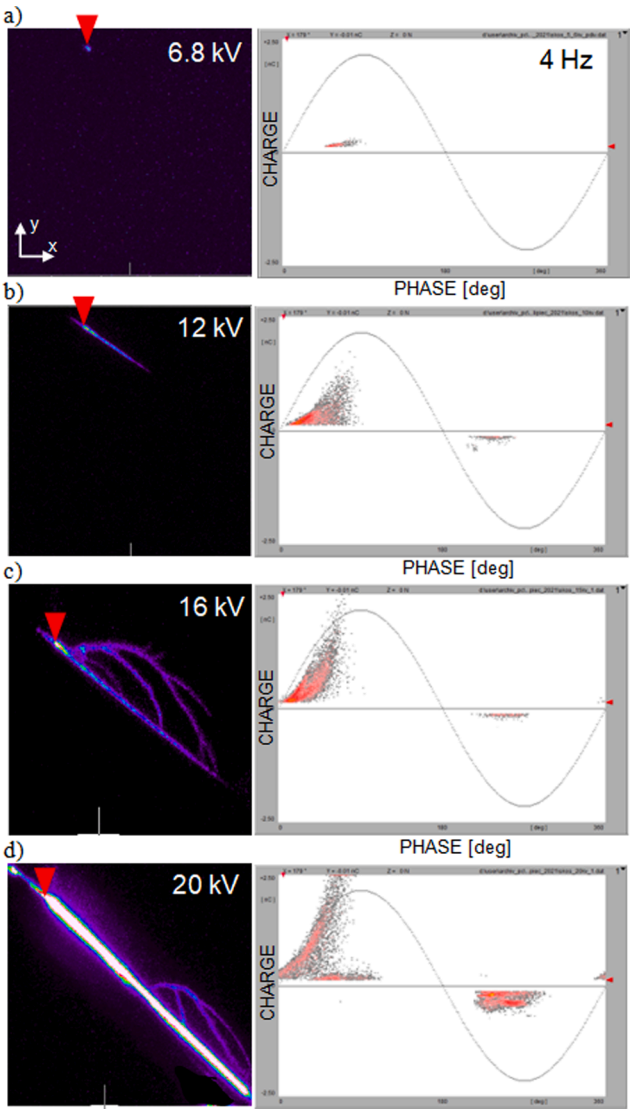

Fig. 6. Optical streamer imaging (left) and corresponding PD phase-resolved patterns (right) as function of applied voltages: a) 6.8 kV; b) 12 kV; c) 16 kV; d) 20 kV.

up to 12 kV. The exemplary sequence highlights the strong surface streamers at 20 kV that are associated with the airborne streamers that are triggered by a surface spot at a certain distance from the HV electrode. The rise of the voltage results in the prolongation of a streamer channel (visible in Fig. 6a-d); the higher the voltage, the further the airborne streamer starts from the electrode. The applied voltage influences the streamer length along the dielectric surface as well as the pathway of the airborne one.

A visualization of the evolution of the surface streamer's length (L, in arbitrary unit) along the dielectric surface is shown in Fig. 7 for voltages of 6.8 through 20 kV at the tip of the high-voltage electrode. The voltage-dependent exemplary discharge span (L) along the dielectric surface is shown in Table 1. The length L indicates the maximum length recorded at certain voltage. The length of the surface streamer grows from 10 au at an inception voltage of 6.8 kV through 96 au at 12 kV up to 203 au at 20 kV.

5. Streamer simulation model

The presented model reflects a positive streamer configuration in a strong non-uniform electric field in gas. The intent of the simulation was to interpret the airborne streamer's appearance that originated at a distance from the HV electrode and influenced a hypothetical accumulated surface charge spot. The 2D geometry used for the simulation is presented in Fig. 8. The inclined dielectric plate is positioned between the high-voltage needle electrode (diameter – 100 μm; radius of curvature – 50 μm) and sticks to the surface and grounded plane. The boundary conditions are indicated in the graph: the high-voltage potential on the needle electrode (anode), and the plate electrode is grounded (cathode). The zero charge density is set at the boundaries. The spot of the accumulated surface charge is indicated. The tiny surface spot was modelled as a flat line, 0.1 mm long, placed on the surface with a defined surface charge density. The simulations were performed in the COMSOL Multiphysics environment using the plasma physics module [60].

The standard (STP) temperature of 300 K and pressure of 1 bar were assumed in the simulations. The gas was simulated by abstract atoms A. The initial concentrations of the electrons and positive ions are equal to 10^{16} m^{-3}; for the negative ions, this is set to zero. In this paper, background ionization was applied as an alternative approach to simulating photoionization and this term is impacting and overriding the regular initial conditions [12,50,52].

The modeling of the streamers combines the effect of the background electric field and space charge field created by the streamer itself. The model presented in this paper solves the electron and ion continuity and momentum equations in the drift diffusion approximation and coupled with Poisson's equation [60]. The local electric field approximation denotes that the transport and source coefficients were parameterized by a reduced electric field (E/N, where E is the electric field, and N – the gas concentration). The following set of equations that govern the motion, generation, and recombination of the three species (i.e., electrons as well as negative and positive ions) were applied. Space charge density q_s results from the net sum contribution of the n_e electrons and both the n_p positive and n_n negative ions, taking their polarity into account:

$$q_s = e(n_p - n_n - n_e), \tag{1}$$

where e is an elementary charge.

Potential V is calculated from the Poisson equation:

$$\nabla\cdot(\varepsilon_0 \nabla V) = -(q_s + \rho_d), \tag{2}$$

where ε_0 is a vacuum dielectric permittivity, ρ_d is the surface charge density, and electric field $\boldsymbol{E}$ is a gradient of potential V:

$$\mathbf{E} = -\nabla V \tag{3}$$

The rate of change of electron density n_e is governed by the drift–diffusion equation [59,61]:

$$\frac{\partial n_e}{\partial t} + \nabla\cdot\Gamma_e = R_e, \tag{4}$$

where R_e is a source coefficient that is related to the electron-generation and -recombination processes. Electron flux vector Γ_e is denoted as follows:

$$\Gamma_e = \mu_e n_e \nabla V - \nabla(\mathbf{D}_e n_e), \tag{5}$$

where μ_e is the electron mobility, and $\boldsymbol{D}_e$ is the electron diffusivity.

The electron mobility is defined by a function [60]:

$$\mu_e = 3.74\cdot10^{24}\cdot(E\cdot10^{21})^{-0.22}\ [V\cdot s\cdot m]^{-1}. \tag{6}$$

The source coefficient R_e is determined by plasma chemistry and the Townsend coefficient [60]:

$$R_e = \sum_{j=1}^{M} x_j \alpha_j N_n |\Gamma_e|, \tag{7}$$

where M represents the number of reactions, x_j is the mole fraction of the

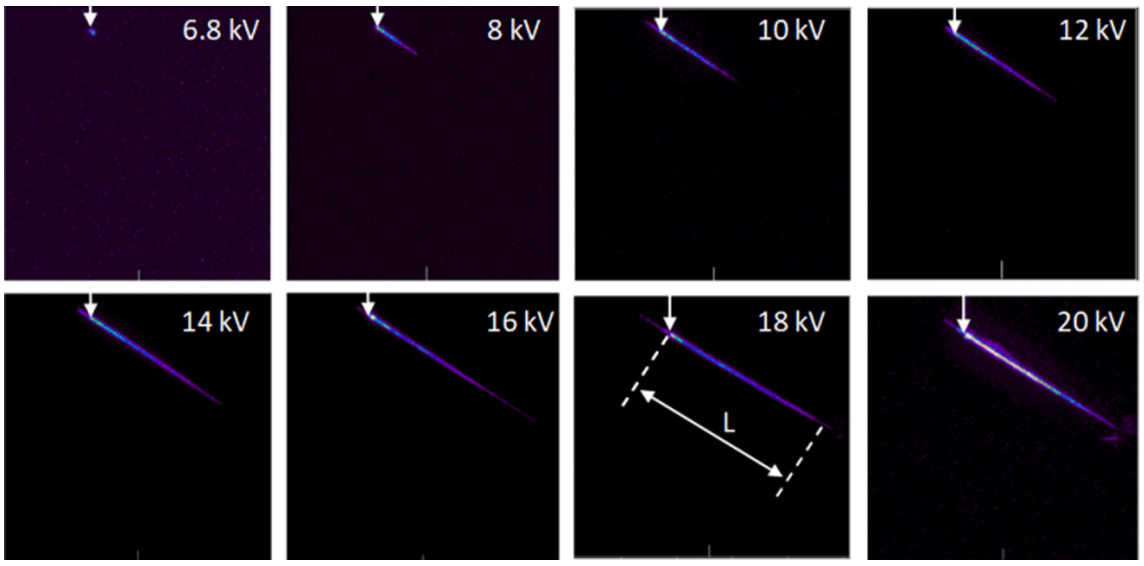

Fig. 7. Evolution of surface streamer length L along dielectric surface with applied voltage within range of 6.8 through 20 kV (a.u. – arbitrary unit).

Table 1
Voltage-dependent discharge span along dielectric surface.

Voltage U [kV]	6.8	8	10	12	14	16	18	20
Length L [a.u.]	10	43	72	96	157	176	186	203

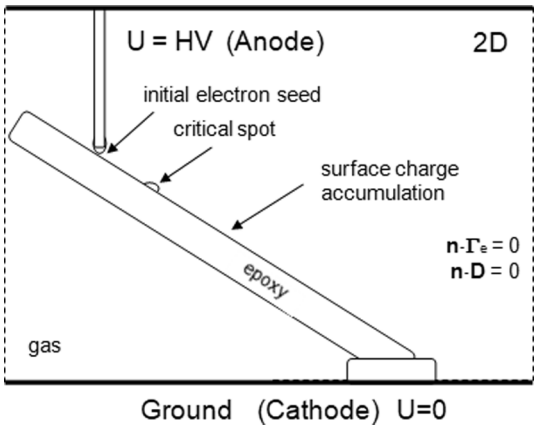

Fig. 8. Configuration of simulation domain.

target species for reaction j, α_j is the Townsend coefficient with respect to reaction j, and N_n is the total neutral number density.

The photoionization was simulated as background ionization with a value of $R_e = 10^{23}$ [12,50].

The diffusion equation for non-electron species in a general form is specified by the following [60]:

$$\rho \frac{\partial w_k}{\partial t} + \rho(\boldsymbol{u}\bullet\nabla)w_k = \nabla\bullet\mathbf{j}_k + R_k + S_p, \tag{8}$$

where $\boldsymbol{j}_k$ is the diffusive flux vector, R_k is the rate expression, S_p is the photoionization component, $\boldsymbol{u}$ is the mass averaged fluid velocity vector, ρ denotes the density of the mixture, and w_k is the mass fraction of the k^{th} species. The reduced mobility of the negative and positive ions is $6{\cdot}10^{21}$ $[V{\cdot}s{\cdot}m]^{-1}$. The following reactions (presented in Table 2) and their corresponding control coefficients were considered:

- impact ionization α,
- attachment of electrons to neutral molecules η;
- recombination of positive and negative;

Table 2
Reaction types (A – abstract atom, e – electron, n – negative ion, p – positive ion).

Reaction type	Reaction formula	Reaction coefficients
Ionization	e + A → p + 2e	Townsend
Attachment	A + e → n	Townsend
Attachment	A + A + e → n + A	k^f
Recombination	e + p → A	k^f
Recombination	n + p → A + A	k^f

- recombination of electron and positive ions;
- rate coefficient k^f.

The coefficients used for the simulations were adopted from the research papers from [11–13,27,60–62].

To initiate a discharge, a kernel of a seed charge (electrons and positive ions) that reflected a Gaussian distribution was placed in front of the tip of the HV electrode:

$$n_{e0} = n_{e0max} exp\left[-\frac{(x-x_0)^2}{2s^2} - \frac{(y-y_0)^2}{2s^2}\right] + n_{e0min} \tag{9}$$

with the following parameters: $n_{e0max} = 10^{16}$ m^{-3}; $n_{p0min} = 10^{13}$ m^{-3}; $n_{np0max} = 10^{16}$ m^{-3}; and s = 200 μm.

The surface process was simulated in a twofold manner; first, no initial surface charge was assumed, and the accumulated charge level was estimated – this value created a rough estimate of this possible surface charge accumulation; second, this value was assumed as an initial surface charge that was concentrated on a spot for airborne triggering and compared with a critical value that initiated the streamer from the spot. The accumulation of surface charges is described by the difference in the normal component ($\boldsymbol{n}$) of the dielectric displacement between dielectric $\boldsymbol{D}_d$ and gaseous side $\boldsymbol{D}_g$ and results in surface charge density ρ_d:

$$\rho_d = \mathbf{n}(\mathbf{D}_d - \mathbf{D}_g), \tag{10}$$

and considering material permittivity ε_r:

$$\rho_d = \mathbf{n}\varepsilon_0(\varepsilon_r\mathbf{E}_d - \mathbf{E}_g) \tag{11}$$

The dynamics of surface charge ρ_d is governed by a superposition of the current components that are attributed to the electrons and both the negative and positive ions, denoted as $\boldsymbol{J}_e$, $\boldsymbol{J}_n$, and $\boldsymbol{J}_p$, respectively:

$$-\frac{\partial \rho_d}{\partial t} = \boldsymbol{n}\boldsymbol{J}_e + \boldsymbol{n}\boldsymbol{J}_n + \boldsymbol{n}\boldsymbol{J}_p \quad (12)$$

The significant phase of the simulations is the mesh adjustment. A non-uniform triangular mesh was used. Certain groups were distinguished, such as the electrode edges and the streamer development area (where the maximum element size was tuned to 8 μm). The simulation environment of the PARDISO in COMSOL Multiphysics solver was used.

The aim of the simulations was to demonstrate the appearance of an individual airborne streamer that was triggered away from the HV tip due to the surface charge accumulation that was caused by the previous streamers. The presented simulations were performed with DC voltage at a high-voltage electrode that was equal to U = 30 kV. Since the propagation of an individual streamer is within a time range of nanoseconds, the DC condition can be assumed for the simulation (mimicking a time slot on the sinusoidal waveform). Assuming the localized surface charge spot at a distance from the electrode tip, the simulations of the streamer propagation were carried out. In the first step, the streamer propagation in the 'clean' environment without a prior accumulated charge ($\sigma_d = 0$) on an epoxy surface was carried out. The electron density N_e and electric field development at 5 ns are shown in Fig. 9. The streamer starts from the HV electrode tip side (Fig. 9a) and propagates along the dielectric surface. Since a positive (cathode-directed) streamer deposits positive charges on the surface, one can imagine an accumulation of the charge with a certain density profile after several repetitions. The electric field distribution around the streamer channel at 5 ns is shown in Fig. 9b. The tiny cathode sheath was observed as outlined in [13].

The assumed value of the charge accumulation on the dielectric surface was at a level of $5{\cdot}10^{-4}$C·m^{-2}. According to the hypothesis, the airborne streamer was triggered from the accumulated surface charge spot in this case. The spot is located at a coordinate of $x = 1.9$ mm. The corresponding electron density N_e and electric field distribution are shown in Fig. 10. A tiny inception is visible around the HV electrode tip; however, the main airborne streamer is triggered at the accumulated charge spot location in this case (Fig. 10a). The electric field distribution around the airborne streamer channel at 2 ns is shown in Fig. 10b. A

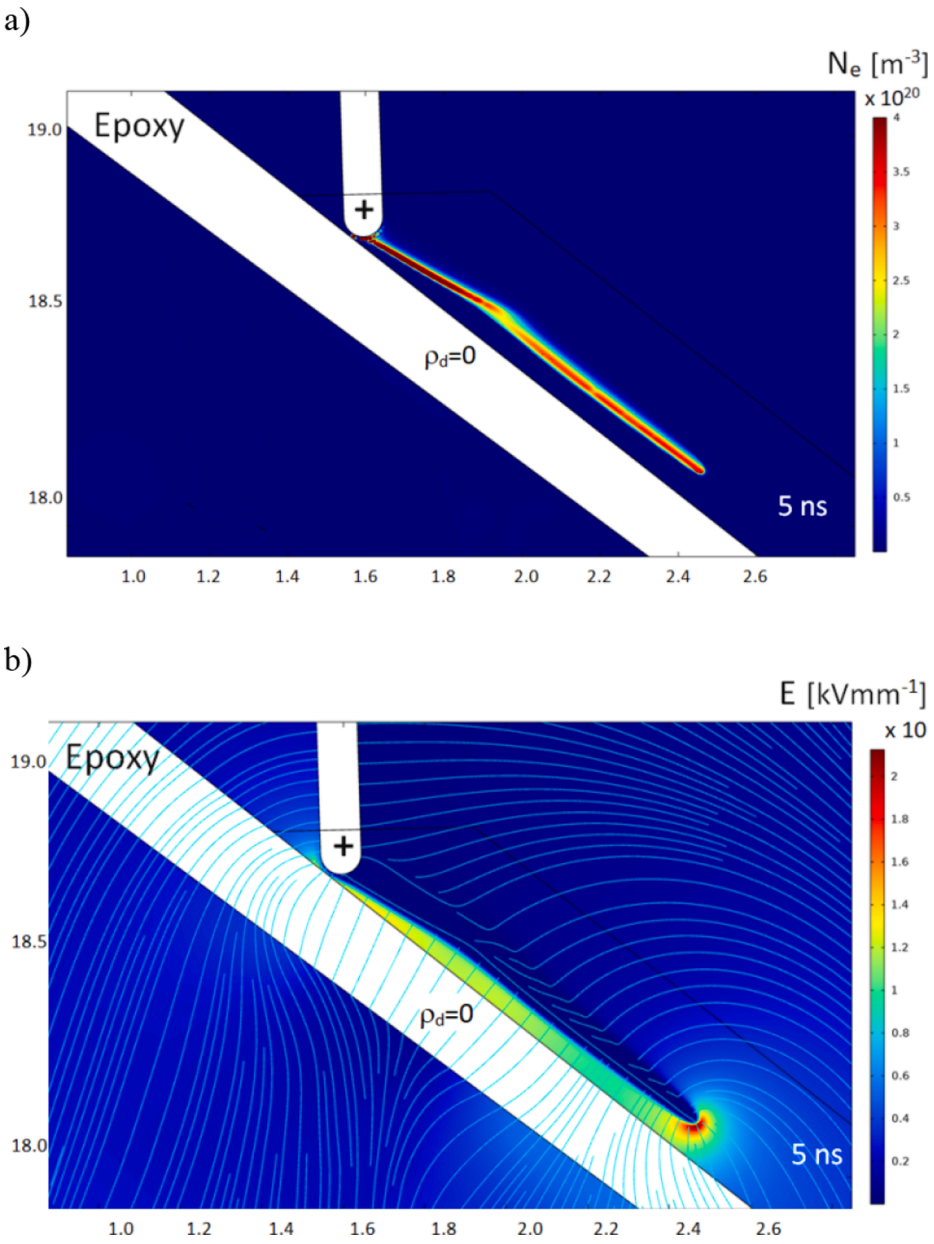

Fig. 9. Streamer development adjacent to dielectric surface without prior accumulated charge: a) electron density N_e; b) electric field distribution.

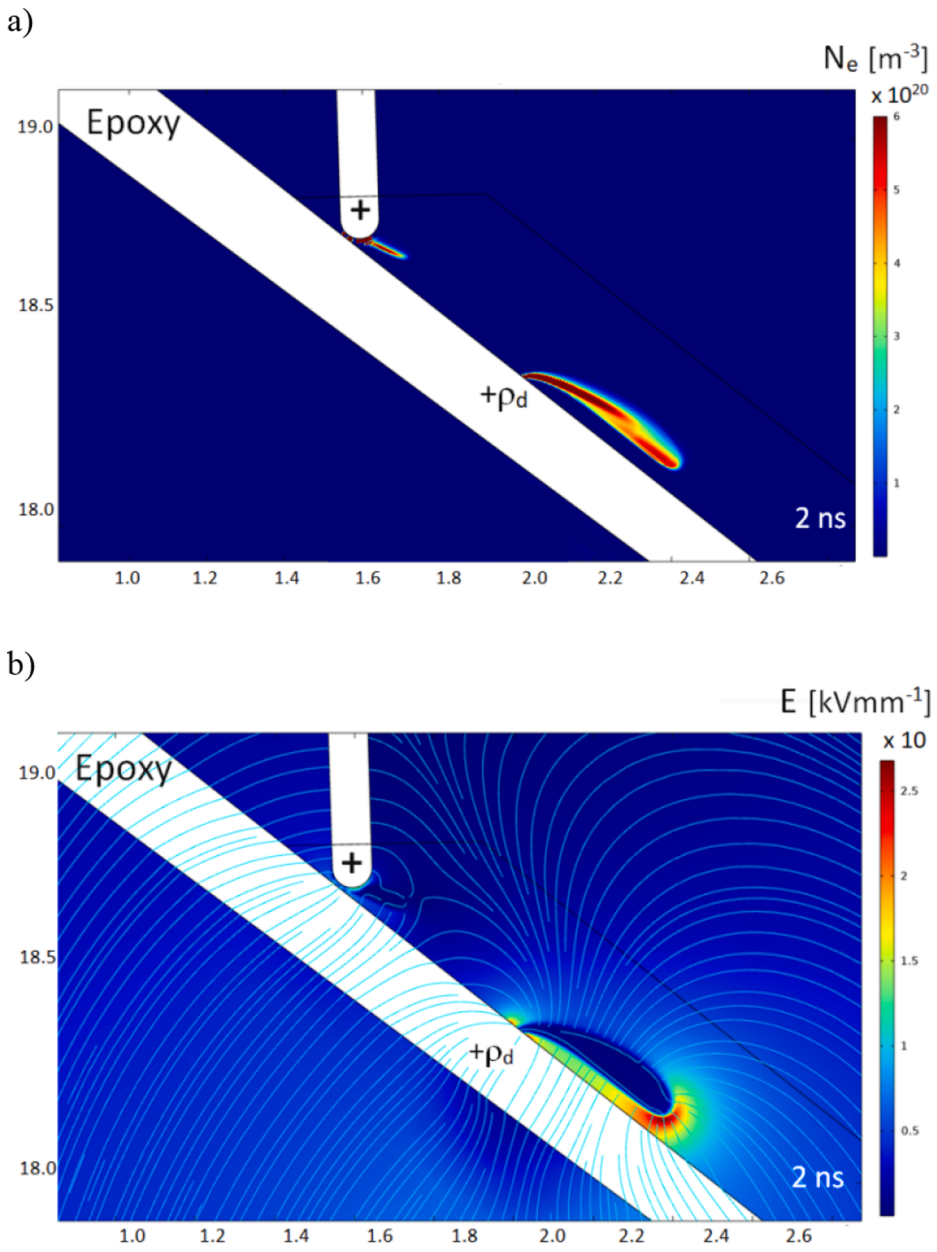

Fig. 10. Streamer development adjacent to dielectric surface with presence of accumulated charge spot located at coordinate of x = 1.9 mm: a) electron density N_e; b) electric field distribution.

strong electric field is observed at the streamer head.

As it is commonly known, the breakdown strength of air is equal to $E_b = 3$ kV·mm^{-1}, hence the resulting density of surface charge will correspond to $\sigma_d = \varepsilon_0 \cdot E_b$, which gives a critical value of $2.7 \cdot 10^{-3}$C·m^{-2}. Thus the value of surface charge density assumed in simulations is above the streamer inception level and below the value which is causing breakdown in air. In this way a critical value assumed for simulations, leading to the streamer inception and propagation, is below the value corresponding to the electric breakdown in air. In the presented measurements and simulations the streamer is not leading to the breakdown. The focus was on the distinction between the airborne and surface streamers. In this context, observed phenomena will be triggered in the presence of local spots with high-charge densities.

As a streamer will develop lengthways the electric field lines, the accumulated surface spot will trigger the deflection of the streamer path. This process is visualized in Fig. 10 (which depicts the electron density and electric field distribution). The pathway trajectories of the airborne streamer need further investigations in the future with respect to the dielectric material properties and the variation of the charge density of the accumulated spot (including the charge decay effect). The accumulated surface charge will influence the electric field distribution. The comparison of a case without a surface charge (Fig. 9) and one with an accumulated surface charge (Fig. 10) reveals different streamer propagation behaviour.

6. Discussion

The inspiring effect in the presented research was the appearance of airborne streamers in the imaging in certain sequences for the cathode-directed streamer configuration that was adjacent to a dielectric surface. Most of the cathode-directed streamers propagated along the dielectric surface. The attraction effect of the positive streamers to the dielectric surface has been presented in several publications [32,33]. This effect is dependent on the electric permeability of the dialectic material, which

influences the velocity of the surface streamer propagation [13]. However, the interesting observation reported in this paper refers to the coexistence of those airborne streamers that occur between the sequences of surface ones. The presented effect is attributed to the hypothesis of the accumulation of surface charges from the subsequent streamer events reaching a certain critical value at which the airborne streamer is triggered at a distance from the HV electrode. The observed streamer jump from the surface-adjacent propagation might have various origins; it may be related to the charge accumulation on the surface, thermal effects, the interplay of an electrical withstand of air versus the surface effects, etc. The first hypothesis is elaborated further in this paper. The occurrence of the airborne effect just at the tip of the high-voltage electrode is understandable since the occurrence of either a surface or airborne streamer depends strongly on many factors (including the spot of the electron seed, etc.) and also has a statistical character. What was intriguing was the observation of airborne streamers at some distances from the HV electrode (Fig. 5b). Such streamers were suddenly detached from the surface, revealing the flight part in the gaseous segment.

It is assumed that the surface streamers charge the surface and that the cumulative charge spot occurs at a certain position that is related to the average streamer propagation length. The charging effect may have multiple causes, such as photoemissions (electrons emitted from the surface due to high-energy photons), the deposition of positively charged molecules along the streamer channel length behind the head, or the polarization of the dielectric material due to the Lapplacian field in the electrode setup. Reaching a certain critical value, the incoming consecutive streamer enhances the local electric field that is composed of the superposition of the Lapplacian field, the field coming from the space charges and surface charges, and the dynamic field modification due to the presence of the streamer profile. At this point, the spot of the accumulated surface charge starts to trigger a new streamer that propagates vertically or at a certain angle relative to the surface along the electric field lines.

The pathway of this streamer is visible – like the bubble on the recorded imaging from the side view. The surface is positively charged by both the ions that are deposited by the streamer channel and the surface positive polarity due to the deficiency of the electrons that were involved in past streamer formations. This potential charge accumulation is visualized in Fig. 11. The positive streamer propagation direction (from anode to cathode) is marked, and several streamers in consecutive time events t_1, t_2,…t_n are indicated. In the case of the positive streamer, the outer layer (indicated by the red contour) is formed by positive ions, whereas a high electron concentration is also present at the streamer head (blue) during the propagation.

The enhanced electric field of the surface streamers was demonstrated in [13]. This was attributed to the electrostatic effects as well as reduced channel radii as compared to the gas streamers. In case of the positive streamers, a higher velocity when compared to the bulk gaseous ones was also computed [33].

At the defined voltage, the streamers propagate along the dielectric surface up to a certain distance; the head has a statistical variation around a position defined as x_σ, forming a certain distribution (one side is skewed). Several iterations of subsequent streamers charge the surface. The deposited positive ions are also repealed electrostatically from the anode. Hence, the accumulation of the surface charge is graphically denoted in Fig. 11 by a symbolic red point with a surface charge density $+\sigma$ localized at the x_σ coordinate and spread with a distribution profile.

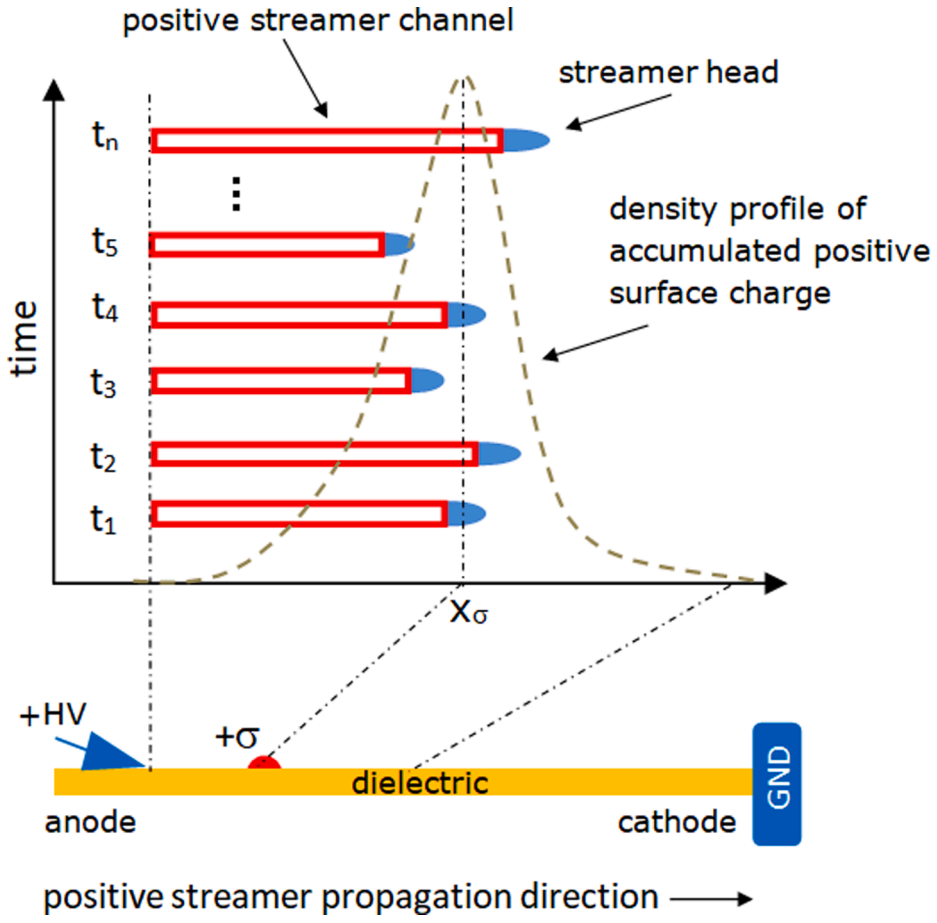

Fig. 11. Sequence of positive streamers adjacent to dielectric surface: $+\sigma$ – surface charge density at accumulation spot; x_σ – localization of spot maximal charge distribution.

Several iterations charge the surface and accumulate the spot charge to a level that a certain subsequent incoming streamer faces the deflection along the electric field lines (forming the airborne channel). It is worth noticing that the airborne streamer occurs during each period of the half-voltage. Thus, this effect can be attributed to the charge accumulation time. The effect is also frequency-dependent and, thus, related to the surface charge decay. It was assumed that the negative half-period did not significantly influence this process since no streamers were noticed in the imaging in this part of the waveform (only glowing around the negative polarized electrode). The experiments were carried out at the sinusoidal voltage with a frequency of 4 Hz; however, the voltage can be treated as a constant for an individual streamer that propagates within nanoseconds. The increasing voltage along the sinusoidal waveform results in the variation of the surface streamer profile and the defection of the airborne ones (as illustrated in Fig. 12). The visualization hypothesis of the airborne streamers' origins with respect to the applied voltage (U_1, U_2) and the location spot of the surface charge accumulation (x_σ) is depicted. The higher voltage results in moving the position of the critical surface charge accumulation spot further away from the HV electrode tip ($x_{\sigma 2}$,> $x_{\sigma 1}$), as was observed in the measurements. This corresponds to the voltage-dependent surface streamer length that is shown in Fig. 7.

The streamer effects along the surface-adjacent propagation at the positive half-period of the high voltage are denoted in Fig. 13. The surface and two airborne streamers are pinpointed. In the case of the airborne ones, the first originates from the HV electrode, and the second from the distantly located charge spot. In the first phase after the voltage reaches the inception level, the ionization will start at around the tip of the HV electrode, resulting in a cloud of positive space charges. The ionization zone will then move down along the surface, as the streamer channel might be perceived as a prolongation of the tip. Two kinds of streamers may propagate from the tip; i.e., a surface-adjacent streamer, and an airborne one (depending on the inception conditions at the tip and the statistical seed effects). The positive surface streamers that slide along the surface deposit positive charges from the channel on the surface, whose density reaches a certain critical concentration at a spot that

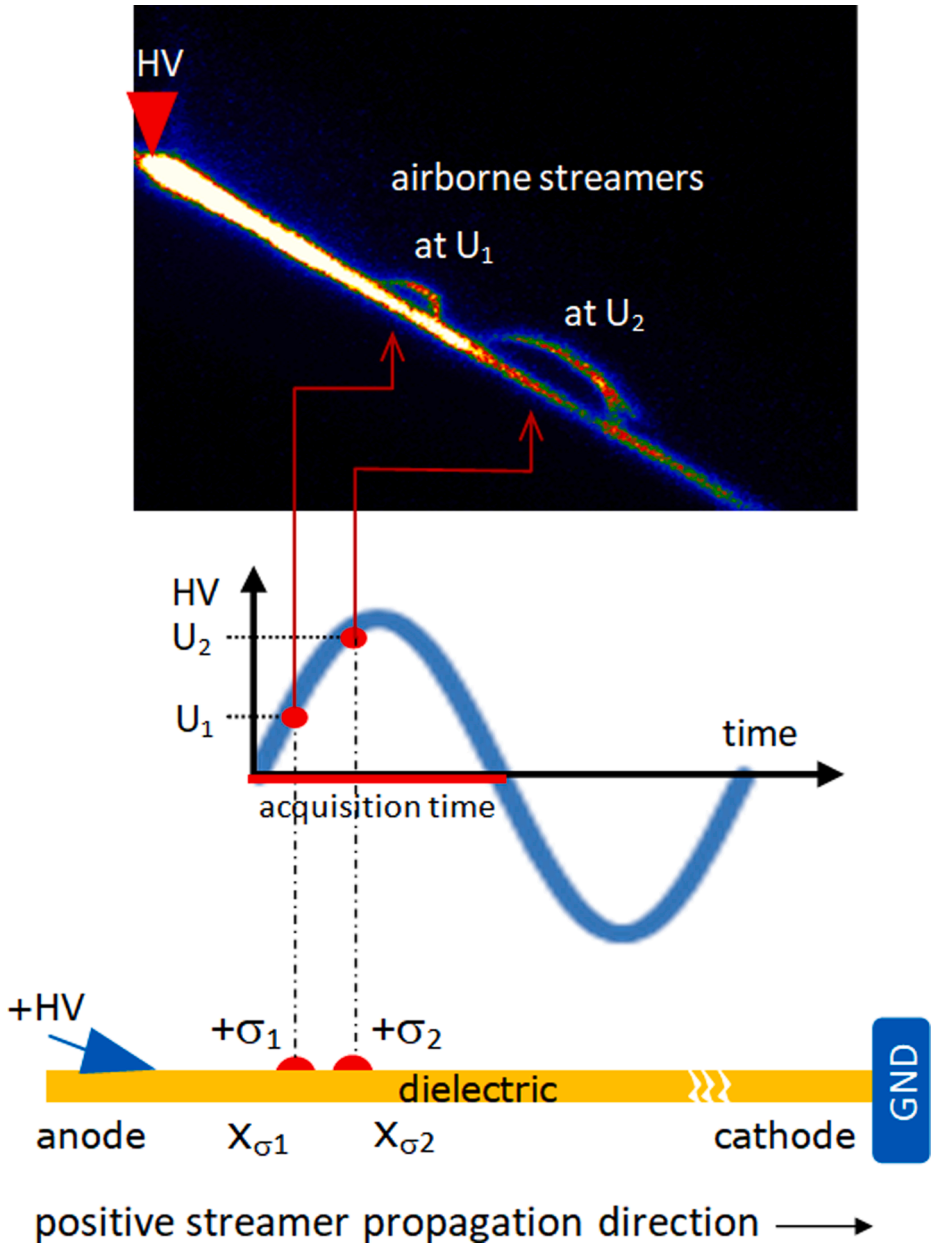

Fig. 12. Visualization of airborne streamers' origins with respect to applied voltage (U_1, U_2) and location spot of surface charge accumulation (x_σ).

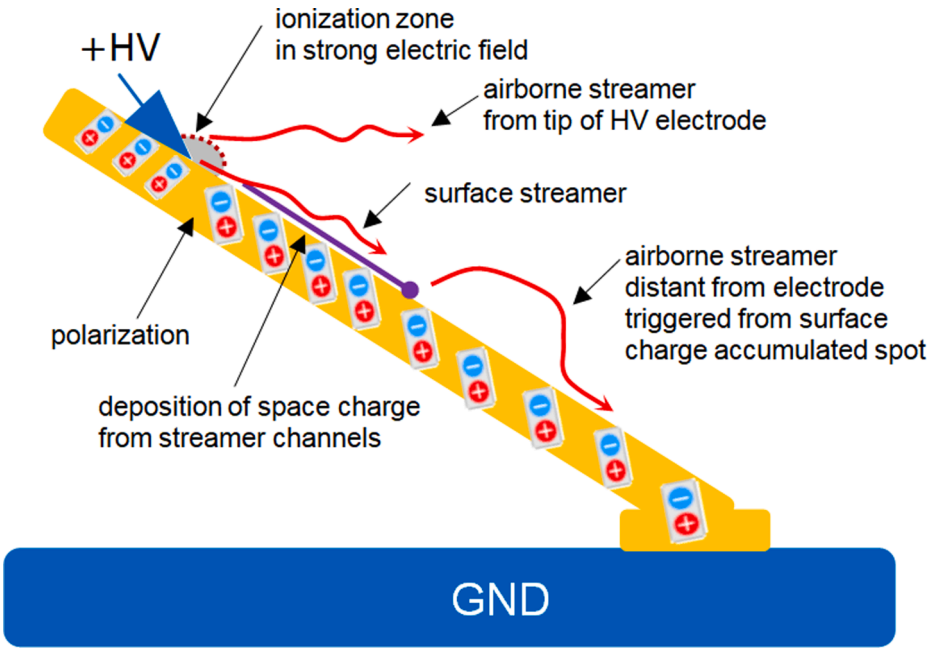

Fig. 13. Illustration of propagation of surface and airborne streamers at positive half-period of high voltage. Surface and two airborne streamers are pinpointed (airborne originating from HV electrode, and distant located at charge spot).

is distinctly located away from the electrode (being an origin of airborne streamers). At this spot, the electric withstand in air is exceeded. The dielectric polarization in the Laplacian electric field (denoted in Fig. 13) along with the streamer photoemission effects on the surface result in the positive surface charge accumulation.

The dynamics of the process depend on the surface's material properties (such as conductivity), which will influence the charge decay times and development of the subsequent streamers [40,42,43,45,46]. The presented hypothesis of airborne streamer inception from an accumulated charge spot on an dielectric surface has also been evaluated by the simulation scenario. The airborne streamer triggering that originates from the critical spot is obtained for a charge density that is equal to $5{\cdot}10^{-4}\mathrm{C{\cdot}m^{-2}}$.

Future investigations and research will comprise the impact of surface material permittivity on streamer propagation, the attraction and repealing effects, and an airborne streamer deflection profile analysis.

7. Conclusion

This paper presents the imaging and simulations of positive airborne and surface streamers in air. The experiments were performed in a configuration with surface discharges that were adjacent to the dielectric. The high-voltage frequency was adjusted to obtain the continuous imaging of streamers over consecutive half-periods without gaps or delays. The goal of this paper was to investigate the intriguing observation of the occurrence of airborne streamers that originate at a dielectric surface at a distance from the tip of an HV electrode. This effect is attributed to the accumulation of a charge at a spot on an epoxy resin plate during subsequent streamers. After reaching the critical value of the charge density, such a positively charged spot causes airborne streamer inception. The effect can be observed in a side view by high-speed imaging in a time-accumulated and spatially resolved mode. Especially important was to record streamers in consecutive periods of the high voltage without a gap needed for camera data streaming. The frequency of the high voltage was tuned to 4 Hz to obtain a continuous gapless sequence of surface discharges.

The occurrence of streamer discharges was also detected electrically using phase-resolved acquisition within a half-period of the applied voltage. The hypothesis of the occurrence of airborne streamers in certain sequences was complemented by 2D simulations using COMSOL's Plasma module. Two types of streamers were simulated: the first – without an accumulated surface charge; and the second – with a spot of a defined charge density (triggering an airborne streamer). The measurements reflect the presence of these two types of streamers. The airborne streamer was attributed to the surface polarization. The sequence of recorded streamers was presented, illustrating the occurrence of airborne ones every some period. Special attention was paid to those airborne streamers that originate from a spot on a dielectric surface away from the tip of an HV electrode. It was demonstrated that such a spots, being charged during subsequent cathode-directed streamer events after reaching a critical value of the charge density, may trigger a discharge towards the air side. The length of a surface streamer along a dielectric surface and the deflection of airborne streamers are voltage-dependent. The surface charge accumulation was quantitatively evaluated by simulations. A critical value of a surface charge at a spot, in a given configuration of electric field distribution, was assumed $\sigma_{cr} = 5{\cdot}10^{-4}\mathrm{C{\cdot}m^{-2}}$. This critical value of surface charge density used in simulations is above the streamer inception level and below the value which is causing breakdown in air. Also the experimental part was tuned in this way that the streamer is not reaching the ground electrode. The evolution of a streamer's form and the kinetics of airborne streamer branches are dependent on surface charge density. The influence of the dielectric surface on streamer propagation is a complex problem. Future research may reflect additional surface effects and more in depth physical processes. On one side they may incorporate the morphological status of the surface such as roughness or presence of the humidity in the tiny surface adjacent layer. The other direction may be related to the physical interaction of the streamer with the surface for example to involve and simulate electron trapping and releasing during streamer sliding on the surface. In this way photoemission and photoionization will be modelled more precisely. Additional direction will take into account thermal effects, both in streamer channel and in the surrounding environment, including surface. The presented experimental and simulation results extend the insight to streamer mechanism in configurations with charges accumulated on the dielectric surface – including the inception of an airborne streamer.

CRediT authorship contribution statement

Marek Florkowski: Conceptualization, Methodology, Formal analysis, Validation.

Declaration of Competing Interest

The authors declare that they have no known competing financial interests or personal relationships that could have appeared to influence the work reported in this paper.

Acknowledgments

The author would like to thank Dariusz Krzesniak for his assistance in the measurements as well as Dr. Jose Gregorio, Dr. Jannis Teunissen, and Dr. Xiaoran Li for their valuable discussions.

References

[1] S. Nijdam, J. Teunissen, U. Ebert, The physics of streamer discharge phenomena, Plasma Sources Sci. Technol. 29 (2020) 1–49.
[2] L.B. Loeb, Fundamental process of electrical discharges in gases, John Wiley and Sons, New York, 1947.
[3] H. Raether, Electron avalanches and breakdown of gases, Butterworths, London, 1964.
[4] J.M. Meek, J.D. Craggs, Electrical Breakdown of Gases, John Wiley and Sons, 1978.
[5] Y.P. Raizer, J.E. Allen (Eds.), Gas Discharge Physics, Springer Berlin Heidelberg, Berlin, Heidelberg, 1991.
[6] A.A. Kulikovsky, Two-dimensional simulation of the positive streamer in N2 between parallel-plate electrodes, J. Phys. D: Appl. Phys 28 (1995) 2483–2493.
[7] A.A. Kulikovsky, The mechanism of positive streamer acceleration and expansion in air in a strong external field, J. Phys. D: Appl. Phys 30 (1997) 1515–1522.
[8] A.A. Kulikovsky, Three-dimensional simulation of a positive streamer in air near curved anode, Elsevier, Phys. Lett. A 245 (5) (1998) 445–452.
[9] R. Morrow, J.J. Lowke, J. Phys. D: Appl. Phys, Streamer propagation in air 30 (1997) 614–627.
[10] A.A. Kulikovsky, Positive streamer in a weak field in air: A moving avalanche-to-streamer transition, Phys. Rev. E 57 (6) (1998) 7066–7074.
[11] Y.V. Serdyuk, Propagation of cathode directed streamer discharges in air, Proceedings of COMSOL Conf., Rotterdam (2013).
[12] B. Bagheri, J. Teunissen, U. Ebert, et al., Comparison of six simulation codes for p [ositive streamers in air, IOP, Plasma Sources Sci. Technol. 27 (2018) 1–20.
[13] X. Li, A. Sun, G. Zhang, J. Teunissen, A computational study of positive streamers interacting with dielectrics, IOP Publishing Plasma Sources Sci. Technol. 29 (2020) 1–12.
[14] Y. Li, S. Dijcks, G. Sun, J. Wen, Y. Xu, G. Zhang, U. Ebert, S. Nijdam, Characterizing streamer branching in N_2–O_2 mixtures by 2D peak-finding, Plasma Sources Sci. Technol 29 (2020) 1–7.
[15] H. He, D. Xia, B. Luo, W. Chen, K. Bian, N. Xiang, Simulation of positive streamer propagation in an air gap with a GFRP composite barrier, High Voltage (2021) 1–13.
[16] H.A. Ziedana, H. Rezkb, M. Al-Dhaifallahd, A. Elnozahya, An experimental implementation and testing of the corona discharge in wire-duct electrostatic precipitators affected by velocities of incoming flow gases, Elsevier, Measurement 177 (2021), 109296.
[17] Y. Maa, J. Hua, X. Gaoa, N. Liu, Understanding the dependence of streamer initiation on hydrometeors size using Raether-Meek criterion, Elsevier, J. Electrostatics 112 (2021), 103602.
[18] T.M.P. Broels, J. Kos, E.M. van Veldhuizen, U. Ebert, Circuit dependences of the diameter of pulsed positive streamers in air, J. Phys. D: Appl. phys. 39 (2006) 5201–5210.
[19] T. Hoder, H. Hoft, M. Kettlitz, K.D. Weltmann, R. Brandenburg, Barrier discharges driven by sub-microsecond pulses at atmospheric pressure: Breakdown manipulation by pulse width, Phys. Plasmas 19 (2012) 1–4.
[20] G. Wormeester, S. Nijdam, U. Ebert, Feather-like structures in positive streamers interpreted as electron avalanches, Jpn. J. Appl. Phys. 50 (2011) 08JA01.
[21] D.J. Trienekens, S. Nijdam, U. Ebert, Stroboscopic images of streamers through air and over dielectric surfaces, IEEE Trans. on Plasma Sciences 42 (2014) 2400–2401.
[22] S. Mirpour, A. Martinez, J. Teunissen, U. Ebert, Distribution of inception times in repetitive pulsed discharges in synthetic air, Plasma Sources Sci. Technol 29 (2020), 115010.
[23] X. Liua, X. Wanga, X. Zhaoa, P. Xiaob, Y. Liua, J. He, An improved inversion algorithm to reconstruct 2D temperature fields of long sparks with high-speed schlieren technique, Elsevier, Measurement 180 (2021), 109620.
[24] Kosuke Tachibana, Takahiro Koshiishi, Takashi Furuki, Ryuta Ichiki, Seiji Kanazawa, Takehiko Sato, Jerzy Mizeraczyk, A new measurement method of DC corona-discharge characteristics using repetitive ramp and triangular voltages, Elsevier, J. Electrostatics 108 (2020) 103525, https://doi.org/10.1016/j.elstat.2020.103525.
[25] Chathan Cooke, Alan Cookson, The nature and practice of gases as electrical insulators, IEEE Trans. Electr. Insul. EI-13 (4) (1978) 239–248.
[26] S. Nijdam, E. Takahashi, A.H. Markosyan, U. Ebert, Investigation of positive streamers by double-pulse experiment, effects of repetition rate and gas mixtures, Plasma Sources Sci. Technol. 23 (2014) 1–15.
[27] S. Singh, Y.V. Serdyuk, R. Summer, Streamer propagation in hybrid gas-solid insulation, Conf. on Electrical Insul. and Dielectr. Phenomena, 2015.
[28] Lijun Wang, Xuefeng Ou, Yashuang Zheng, Jie Liu, Xin Lin, Tuo Zhang, Numerical simulations of the SF_6-N_2 mixed gas streamer discharge development process, AIP Adv. 9 (5) (2019) 055320, https://doi.org/10.1063/1.5080960.
[29] J.T. Krile, A.A. Neuber, J.C. Dickens, H.G. Krompholtz, DC flashover of a dielectric surface in atmospheric conditions, IEEE Trans. Plasma Sci. 32 (2004) 1828–1834.
[30] H.C. Miller, Surface flashover of insulators, IEEE Trans. on Electrical Insulation 24 (1989) 765–786.
[31] T.S. Sudarshan, R.A. Dougal, Mechanism of surface flashover along solid dielectrics in compressed gases: A review, IEEE Trans. on Dielectrics and Electr. Insul. EI-21 (1986) 727–746.
[32] I. Gallimberti, G. Marchesi, L. Niemeyer, Streamer corona at an insulator surface, 7th Int. Symp. on High Voltage Engineering ISH'91, Dresden, 1991.
[33] X. Li, A. Sun, J. Teunissen, A computational study of negative surface discharges: characteristics of surface stramers and surface charges, IEEE Trans. Dielectrics Electrical Insulation 27 (2020) 1178–1186.
[34] M. Akyuz, L. Gao, V. Cooray, T.G. Gustavsson, S.M. Gubanski, A. Larsson, Positive streamer discharges along insulating surfaces, IEEE Trans. Dielectr. Electric. Insul. 8 (6) (2001) 902–910.
[35] Frank E. Acker, Gaylord W. Penney, Influence of previous positive streamers on streamer propagation and breakdown in a positive point-to-plane gap, J. Appl. Phys. 39 (5) (1968) 2363–2369.
[36] Shigemitsu Okabe, Phenomena and mechanism of electric charges on spacers in gas insulated switchgears, IEEE Trans. on Dielectr. Electrical Insul. 14 (1) (2007) 46–52.
[37] Junbo Deng, Shigeyasu Matsuoka, Akiko Kumada, Kunihiko Hidaka, The influence of residual charge on surface discharge propagation, J. Phys. D: Appl. Phys. 43 (49) (2010) 495203, https://doi.org/10.1088/0022-3727/43/49/495203.
[38] A. El-Zein, M. Talaat, A. Samir, Positive streamer in gases: Physical approach from low to high energies, Elsevier Vacuum 156 (2018) 469–474.
[39] L. Liu, X. Li, T. Wen, Q. Bo, J. Ma, Q. Zhang, Criteria and propagation processes of electrode initiated and electrodeless initiated discharge in SF_6, Physics of Plasma 26 (2019), 023519.
[40] Marek Florkowski, Barbara Florkowska, Pawel Zydron, Partial discharge echo obtained by chopped sequence, IEEE Trans. Dielect. Electr. Insul. 23 (3) (2016) 1294–1302.
[41] Z. Zhao, J. Li, Repetitively pulses gas discharges: memory effect and discharge mode transition, High Voltage 5 (2020) 569–582.
[42] M. Florkowski, Partial discharges in high-voltage insulating systems – mechanisms, processing, and analytics, ISBN 978-83-66364-75-2, AGH Press, Kraków, 2020.
[43] C. Pan, K. Wu, G. Chen, M. Florkowski, Z. Lv, J. Tang, Understanding partial discharge behavior from the memory effect induced by residual charges: a review, IEEE Trans. Dielectrics Electrical Insulation 27 (2020) 1936–1950.
[44] M. Florkowski, Influence of insulating material properties on partial discharges at DC voltage, Energies 13 (2020) 4305.
[45] Z. Zhao, D.D. Huang, Y.N. Wang, C.J. Li, J.T. Li, Volume and surface memory effects on evolution of streamer dynamics along gas/solid interface in high-pressure nitrogen under long-term repetitive nanosecond pulses, Plasma Sources Sci. Technol. 29 (2020) 1–23.
[46] J. Teunissen, A. Sun, U. Ebert, A time scale for electrical screening in pulsed gas discharges, J. Phys. D: Appl. Phys 47 (2021) 1–7.
[47] Xiaobo Meng, Hongwei Mei, Liming Wang, Zhicheng Guan, Jun Zhou, Characteristics of streamer propagation along insulation surface: quantitative influence of permittivity and surface properties, IEEE Trans. on Dielectr. and Electr. Insul. 23 (5) (2016) 2867–2874.
[48] S. Nijdam, J. Teunissen, E. Takahashi, U. Ebert, The role of free electrons in the quiding of positive streamers, IOP Plasma Sources Sci. Technol. 25 (2016) 1–13.
[49] G. Wormeester, S. Pancheshnyi, A. Luque, S. Nijdam, U. Ebert, Probing photo-ionization: simulations of positive streamers in varying N_2:0_2-mixtures, J. Phys. D: Appl. Phys. 43 (2010) 1–13.
[50] F. Boakye-Mensah, N. Bonifaci, R. Hanna, I. Niyonzima, Implementation of a cathode directed streamer model in air under different voltage stresses, Proceedings of COMSOL Conference Grenoble, France, 2020.
[51] B. Bagheri, J. Teunissen, U. Ebert, Simulation of positive streamers in CO_2 and in air: the role of photoionization or other electron sources, Plasma Sources Sci. Technol. 29 (2020) 1–12.
[52] S. Nijdam, F.M.J.H. Wetering, R. Blanc, E.M. Veldhuzein, U. Ebert, Probing photo-ionization: experiments on positive streamers in pure gases and mixture, J. Phys. D: Appl. Phys. 43 (2010) 1–16.
[53] H.K.H. Meyer, R. Marskar, H. Gjemdal, F. Mauseth, Streamer propagation along a profiled dielectric surface, Plasma Sources Sci. Technol. 29 (2020) 1–10.
[54] A. Sobota, A. Lebouvier, N.J. Kramer, E.M. van Veldhuizen, W.W. Stoffels, F. Manders, M. Haverlag, Speed of streamers in argon over a flat surface of a dielectric, J. Phys. D: Appl. Phys 42 (1) (2009) 015211, https://doi.org/10.1088/0022-3727/42/1/015211.
[55] J. Krile, A. Neuber, J. Dickens, H. Krompholz, Imaging of dielectric surface flashover in atmospheric conditions, IEEE Trans. on Plasma Science 33 (2) (2005) 270–271.

[56] Marek Florkowski, Hyperspectral imaging of high voltage insulating materials subjected to partial discharges, Measurement - Elsevier 164 (2020) 108070, https://doi.org/10.1016/j.measurement.2020.108070.
[57] Marek Florkowski, Dariusz Krześniak, Maciej Kuniewski, Paweł Zydroń, Partial discharge imaging correlated with phase-resolved patterns in non-uniform electric fields with various dielectric barrier materials, Energies 13 (11) (2020) 2676, https://doi.org/10.3390/en13112676.
[58] M. Florkowski, D. Krześniak, M. Kuniewski, P. Zydroń, Surface discharge imaging in presence of deposited space charges in non-uniform electric field at DC voltage, High Voltage, special issue "Partial Discharges at DC" 6 (2021) 576–589.
[59] K.L. Liu, R.J. Liao, X.T. Zhao, Numerical simulation of the characteristics of electrons in bar-plate DC negative corona discharges based on a plasma chemical model, J. Electr. Eng. Technol. 10 (2015) 1804–1814.
[60] COMSOL Plasma ModuleUser's Guide 5.6, 2020.
[61] Guojing Dong, Qingmin Li, Tao Liu, Haoyu Gao, Minhao Zhang, Finite-element analysis for surface discharge on polyimide insulation in air at atmospheric pressure under pulsed electrical stress, High Voltage 5 (2) (2020) 166–175.
[62] COMSOL Application note: Negative Streamer in Nitrogen, 2020.